PROCEEDINGS, 50th Workshop on Geothermal Reservoir Engineering
Stanford University, Stanford, California, February 10-12, 2025
SGP-TR-229

Investigating Enhanced Geothermal Systems Feasibility in a Low-Permeability Sedimentary Formation

N Mitha ANGELINA, Inti Rodriguez HERNANDEZ, Lokesh Kumar SEKAR, Esuru Rita OKOROAFOR

Texas A&M University, Richardson Petroleum Engineer Bldg, 245 Spence St Building 3116, College Station, TX 77843

mithaangela@tamu.edu

Keywords: Sedimentary Formation, EGS, Brazos Basin, RELLIS Campus

ABSTRACT

Geothermal energy is a vital energy resource for the evolving energy mix. This is especially true with the potential inherent in enhanced geothermal systems to harness heat from hot rocks that do not have sufficient permeability and working fluids. This study presents a preliminary evaluation of EGS feasibility in sedimentary formations. We investigate the Schuler formation in the Brazos Basin. This formation is estimated to have temperatures between 200 and 250 ºC. Preliminary petrophysical data indicated that the targeted layers have very low porosity with no natural fractures, low permeability, and no hydrocarbons, thus making them candidates for EGS. This study includes geological modeling, reservoir modeling, and production-reinjection scenarios simulation. We examined the impact of well spacing, well perforation at different levels, number of producers, and production time. Preliminary results indicate that more production wells resulted in better thermal performance. The wells with the same perforation level between the injector and producer resulted in better heat extraction.

1. INTRODUCTION

The growing demand for low-carbon and sustainable energy sources has led to increased interest in geothermal energy extraction (Wu and Li. 2020). Traditional/conventional geothermal systems often rely on high-temperature magmatic heat sources to supply the thermal energy source (Sutra et al., 2021). A geothermal field designated for a power plant must possess certain characteristics, including high porosity and permeability (Lund, 2010), within a depth of 1000 – 3000 m (Bertani, 2006), and having enough and consistent working fluids. Furthermore, a heat source is essential, with research suggesting that temperatures of at least 70°C (Lund, 2016) can be utilized for geothermal energy. Some sites may have adequate temperatures but lack the necessary permeability and working fluid to be utilized as conventional geothermal systems (Santos et al., 2022). In such cases, enhanced geothermal systems (EGS) can address this limitation (Sekar and Okoroafor, 2024). The EGS approach involves extracting heat from hot, low-permeability rock by creating or expanding fractures to improve permeability and then injecting water as a working fluid to capture the heat (Gallup, 2009).

Sedimentary basins are increasingly being targeted for geothermal energy development due to their widespread distribution, favorable thermal gradients, and the presence of highly porous and permeable formations that facilitate fluid circulation (Bielicki et al., 2023). It can provide moderate-temperature geothermal resources at economically viable drilling depths, making them suitable for direct-use heating and power generation (Norden, 2011). Many of these basins already host extensive oil and gas infrastructure, allowing for cost-effective repurposing of existing wells and data to assess geothermal potential (Duggal et al., 2022). Additionally, the presence of deep saline aquifers and naturally fractured reservoirs enhances heat exchange and fluid mobility, key factors in optimizing geothermal production (Pandey et al., 2018). Advances in Enhanced Geothermal Systems (EGS) and closed-loop technologies further improve the feasibility of extracting geothermal energy from sedimentary settings. As a result, sedimentary basins represent a scalable and accessible alternative for expanding geothermal energy deployment in both new and existing energy markets.

One of the key challenges in developing geothermal resources in sedimentary basins is the optimization of well placement and reservoir management to maximize heat extraction efficiency (Zhang et al., 2021). A study conducted by Sun et al. (2024) investigated the effect of well spacing on temperature drop after 30 years of production. The results of this study concluded that longer well spacing will reduce the temperature drop of the reservoir, but when the well spacing is over 600 m, the temperature drop is similar to 600 m well spacing. Apart from well spacing, we hypothesize that variations in perforation depth between the injector and producer wells, along with the number of wells, will also influence the reservoir's temperature decline. Understanding the impact of different well configurations on thermal performance is crucial for designing efficient geothermal extraction strategies.

2. STUDY OBJECTIVE

This study examines the impact of well placement, perforation location, and the number of wells on the thermal performance of EGS production and injection. The objective is to determine an optimal well placement strategy for geothermal energy extraction from a specific site: the Texas A&M University RELLIS Campus. The RELLIS Campus is situated within the Brazos Basin in Bryan, Texas, as illustrated in Figure 1. The Greater East Texas Basin, which includes the Brazos Basin, has been identified as a promising candidate for geothermal development (Weijermars et al., 2018) due to its deep sedimentary sequences and favorable thermal gradients. Within this region, formations such as the Schuler Sandstone and Knowles Limestone present varying degrees of heat retention properties that could influence geothermal energy production potential (Ewing, 2011). Based on offset well data, the Brazos Basin has a geothermal gradient of approximately 37.6°C/km (Weijermars et al., 2018).

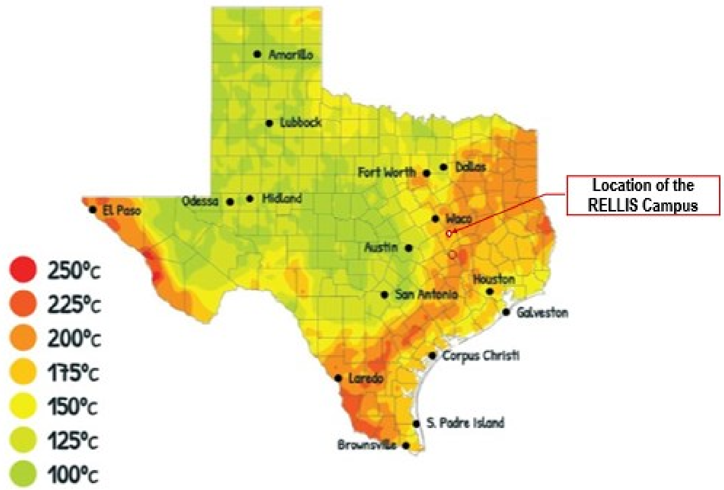

Figure 1: Location of the RELLIS Campus within Texas' temperature profile at a depth of 5.5 km (Blackwell D, 2011)

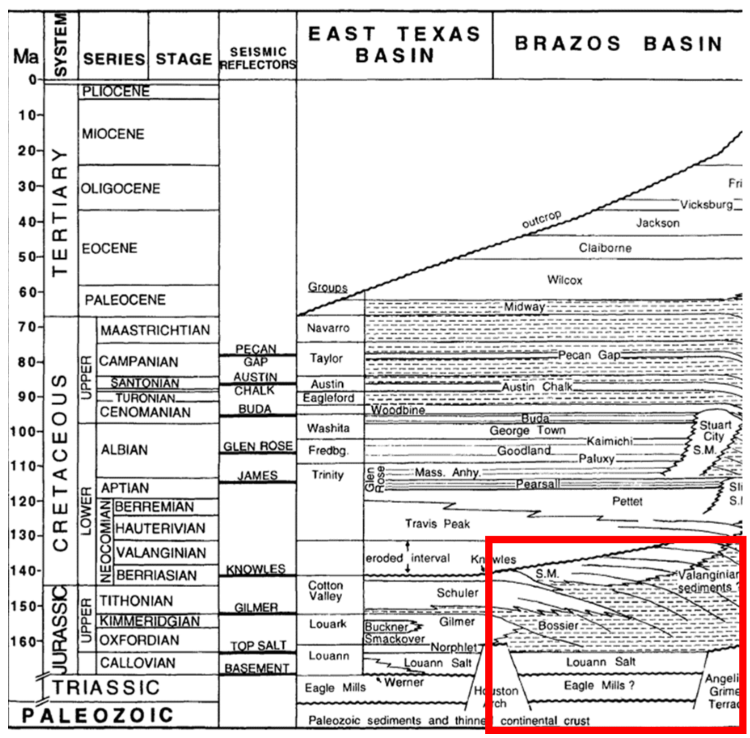

Figure 2. Stratigraphic Correlation Chart of the East Texas Basin and Brazos Basin, Compiled from Various Authors. The Red Square Represents the Formations Under Study (Adapted from Davidoff, 1993)

This study focuses on two formations within the Brazos Basin: the Schuler Sandstone and the Knowles Limestone (Figure 2). According to Davidoff (1993), the Bossier Shale forms the lowermost unit, primarily consisting of prodelta sediments. The Schuler Sandstone, which was deposited concurrently in some areas, represents a transition from open marine to fluvial environments. This regressive sequence is capped by Knowles Limestone, a carbonate ramp deposit characterized by localized patch reef development. These formations belong to the Cotton Valley Group.

3. METHODOLOGY

3.1 3D Geological Model

A three-dimensional model was constructed using the petrophysical and geological properties of existing wells in the Brazos Basin. The overall geometry of the model is detailed in Table 1. The Carrabba 1 well served as the reference well, with its well logs displayed in Figure 3. The petrophysical model indicates that the well intersect four formations: Knowles, Schuler, Gilmer, and Bossier (Figure 4). For simplicity, the formation is assumed to be homogeneous. The porosity and permeability of all formations, except the Knowles formation, are set at 0.01 and 0.1 mD, respectively. The Knowles formation, however, is assigned a permeability of 10 mD. This permeability is used to simulate the effect of hydraulic simulation in the formation, assuming that the average permeability could increase to 10 mD if EGS is applied.

Other properties, such as heat capacity, are also assumed to be homogeneous throughout the entire formation. The reservoir pressure is estimated using an average hydrostatic pressure gradient of 1 Mpa/Km, while the temperature is calculated based on a standard geothermal gradient of 37.6°C/km.

Table 1: RELLIS Reservoir grid parameters

Reservoir Grid Parameters	
Model Units	Metric
Top Depth (TVDSS)	4825 m
Grid cells	1366 x 1801 m x 309 m
Cell dimensions	Dx: 1 m Dy: 1 m DZ: 1.53 m
Total number of cells	13,453,200

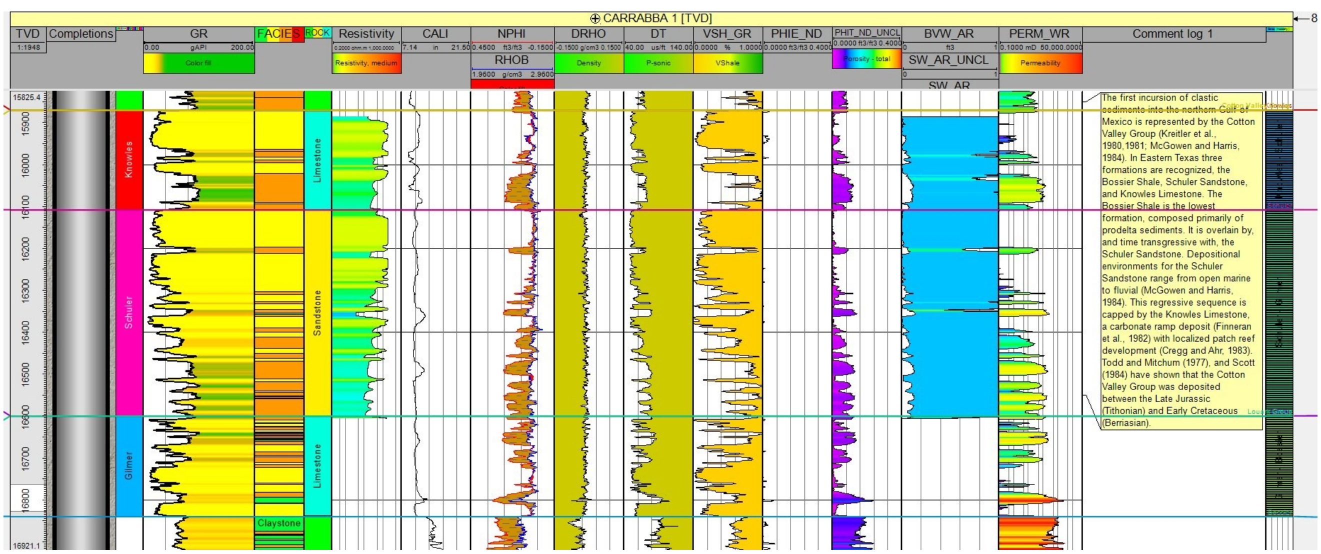

Figure 3. Well logs obtained from existing wells on RELLIS Campus

3.2 Simulation

In this study, a numerical reservoir simulation (thermohydraulic model only) was conducted for five cases, with Case 1 serving as the base case. All cases involve two wells—one injection well and one production well—operating simultaneously from day 1 of the simulation, except for Case 5, where two production wells are placed with one injection well positioned between them. The well locations for these simulations were selected based on the general depth of the reservoir, ensuring uniformity across the reservoir. As shown in Figure 1, the reservoir has both deeper and shallower sections, so to avoid any impact from dip variations, the wells were positioned accordingly (Figure 5). In Case 1, as the base case, the production and injection wells are spaced 150 m apart, with 15 m of perforation at depths of 4969 – 4984 m. Further details for each scenario are provided in Table 2.

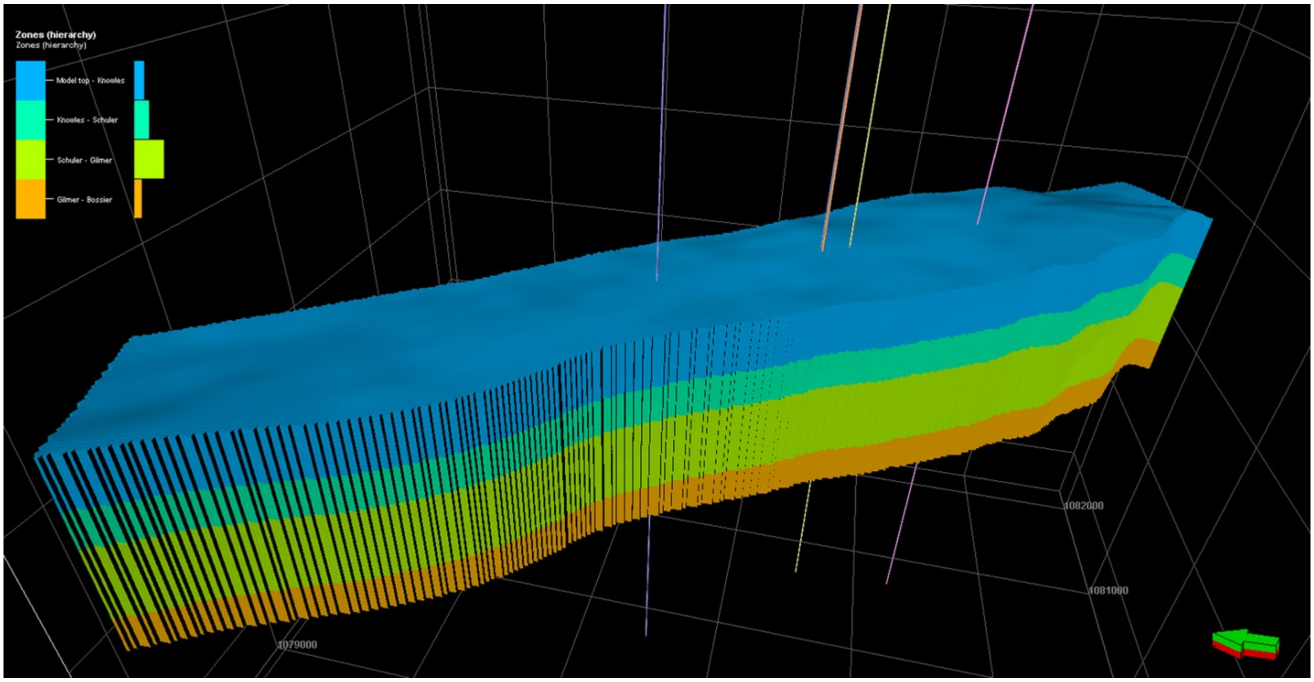

Figure 4: RELLIS 3D geological model

4. RESULTS

This section provides a comprehensive summary of the results obtained from all five cases. The five cases evaluated different well configurations and spacing, revealing variations in temperature behavior and water production rates.

Case 1 serves as the base case for this study. In this scenario, the wells are positioned at the same depth, with a well spacing of 150 m. The temperature of the produced water initially decreases slightly from 208°C to 206°C during the first 20 days of production, then returns to its original temperature and remains stable at 208°C for the next 7 months. After that, the temperature begins to decline exponentially, reaching 178°C by the end of the first year. The water production rate decreases steadily after the first 20 days, then experiences a slight exponential increase starting at month 6, coinciding with the temperature decline, eventually reaching 2,400 m^3/day.

Case 2 features a well spacing of 150 m like case 1 but with the perforations of the two wells positioned at different depths, creating a 60 m depth difference between them, with the injection well located at a deeper level than the production well. The performance of this configuration differs noticeably from Case 1. The temperature of the produced water remains relatively stable at 208°C, with only a slight decrease to 206°C by the end of the first year of production. However, the water production rate declines significantly compared to Case 1. At the end of the first year, the production rate drops to 700 m^3/day in this case compared to 2,400 m^3/day in case 1.

Case 3 features a well spacing of 650 m, with perforations at the same depth level as Case 1. The water production rate remains stable during the first few weeks of production, then begins to decline starting on day 45 gradually. Unlike Case 1, the production rate does not recover, instead continuing to decrease until it reaches 14 m^3/day. The temperature behavior in this case is similar to Case 1, initially dropping after the first day of production, then rising again before starting to decline toward the end of the first year. The key difference between Case 1 and Case 3 is that, after the temperature returns to its initial level, the second fluctuation is smaller, with the temperature only dropping by 2°C. By the end of the first year of production, the temperature of the production well is 206°C.

Table 2: Detail of Scenario 1 to 5.

#Case	Well Perforation Location	Well Spacing (m)	Number of Production Wells	Time of Production (Years)
1	Same Level	150	1	1
2	Different Level	150	1	1
3	Same Level	650	1	1
4	Different Level	650	1	1
5	Same Level	325	2	1

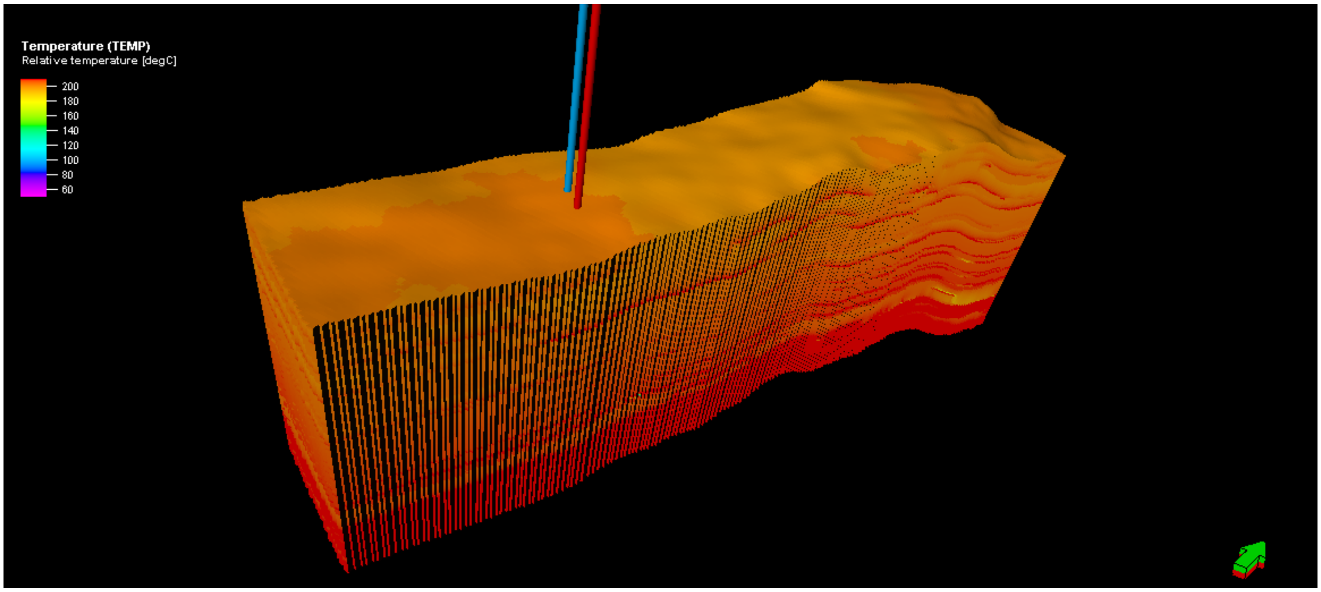

Figure 5: Case 1 scenario's well location. The blue line is the injection well, and the green line is the production well

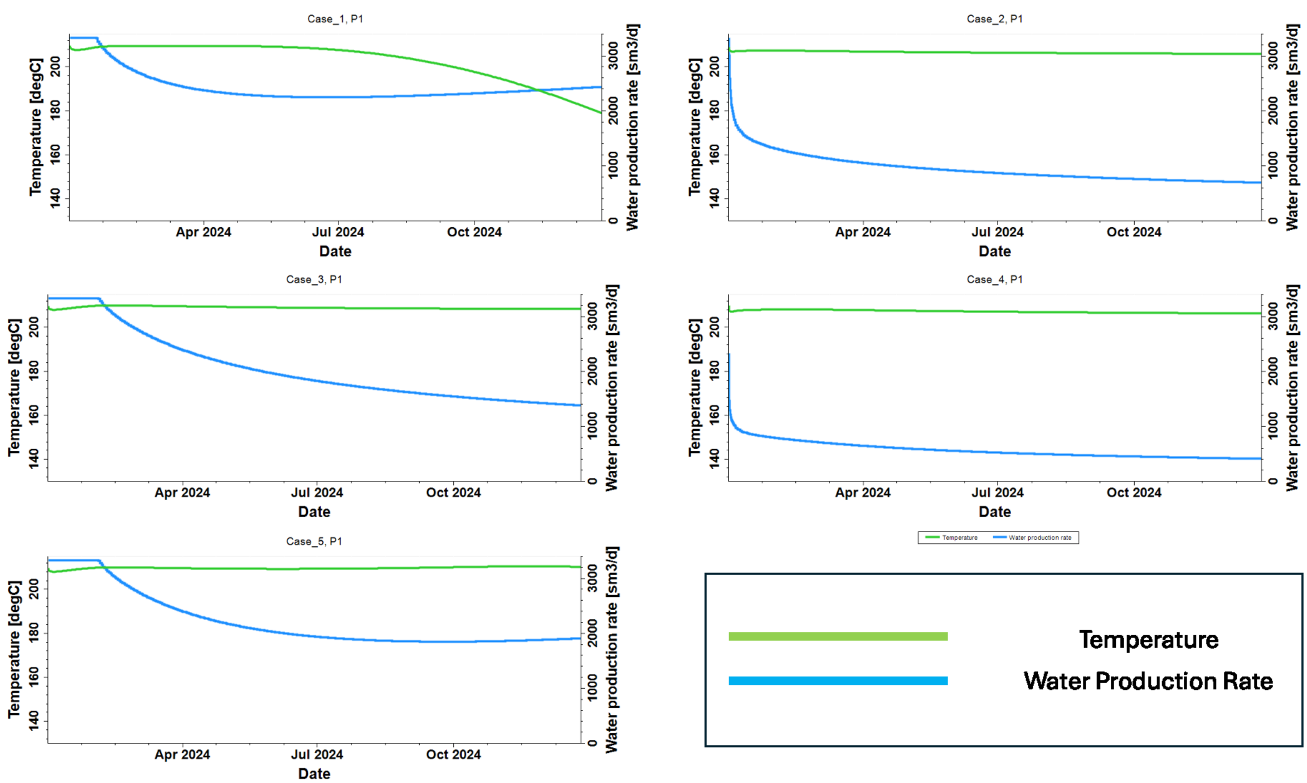

Figure 6: Temperature and water production rate of production well 1 of case 1 to 5.

Case 4 has a well spacing of 650 m, with the production and injection well positioned similarly to Case 3, but with perforations placed at different depths, similar to the configuration in Case 2. In this case, the injection well is located at a deeper depth than the production well, with a 60 m depth difference. The results of this case are generally similar to those of Case 2, with the temperature remaining relatively stable throughout the year, fluctuating between 208°C and 206°C. However, the water production rate drops significantly. The key difference between Case 2 and Case 4 is that the water production rate in Case 4 declines even further, reaching 500 m³/day by the end of the first year.

Case 5 involves two production wells, each with a well spacing of 650 m and identical perforation levels. Between these two production wells is an injection well, positioned at a spacing of 325 m from both production wells. Due to the homogeneous reservoir and the similar well placement of the two production wells, both exhibit identical behavior during the simulation. As a result, only Well P1 is represented in the results. In comparison to Case 1 and Case 3, Case 5 exhibits temperature drop behavior similar to that of Case 3, while its water production behavior mirrors that of Case 1. By the end of the simulation, the water production rate in Case 5 stabilizes at 178°C.

5. DISCUSSION

The results are further analyzed to assess the impact of different well placements, perforation depths, and well configurations on the efficiency of geothermal energy extraction. Additionally, trends observed from each case are discussed to offer a better understanding of the optimal conditions for EGS performance. The temperature and water production rate of production well 1 of cases 1 to 5 is shown in Figure 6.

In **Case 1**, the initial temperature drops on the first day of production were caused by the large volume of water (34,000 m³/day) produced near the wellbore, leading to a rapid pressure drop. This pressure drops caused cooler water from the injector well, located only 150 m away, to flow toward the production well. Since the injected water had a temperature of 18.3°C, it was produced before having enough time to heat up to the reservoir temperature of 208°C. The temperature evolution of Case 1 during different times is shown in Figures 7 and 8.

As shown in Figure 6, the left-hand side depicts the reservoir temperature before injection begins. On starting production and injection, the near-wellbore area cools, while other regions of the reservoir are heated by water from deeper formations with higher pressure and temperature, as seen in the upper right-hand side of Figure 7. Over time, the temperature in the near-wellbore area continues to drop, while the rest of the reservoir heats up until day 11. After 20 days, the water production rate decreases due to the pressure drop from ongoing production, resulting in slower water flow. This allows sufficient time for heat exchange, which gradually raises the temperature of the flowing water in the near-wellbore area closer to its initial temperature, as illustrated on the bottom right-hand side of Figure 6. After day 20, the production well temperature remains constant until month 7, as shown in Figure 8. During this period, from day 20 to month 7, cold water is injected into the reservoir, increasing the volume of cold water within it. This results in reduced heat exchange between the cold water and the surrounding reservoir, causing the cold-water region to expand. Once thermal breakthrough occurs, the temperature of the produced water begins to decrease.

In **Case 2**, where the injector well and production well are perforated at different levels, water tends to flow horizontally. It is unlike Case 1, where the injector well is at the same level as the production well, and the injected water in Case 1 pushes the reservoir water towards the production well, increasing pressure near the well and causing a gradual pressure to drop due to production. In Case 2, however, water cannot flow upward due to gravity and the reservoir dip, preventing most of the injected water from reaching the upper part of the reservoir. Figure 9 illustrates this vertical view, showing that the water from the deeper injector well (lower white box) finds it difficult to flow toward the production well (upper white box), creating a significant drop in the water production rate. The slight temperature decrease in Case 2 is due to the lack of effective heat exchange, as the volume of water flowing is not enough to extract heat from the formation.

In **Case 3**, the water production rate behavior is similar to that of Case 1. In Case 1, due to the short distance between the wells, water breakthrough occurs quickly, which causes the production well to lose pressure. The significant temperature drop in Case 1 is evidence of this water breakthrough. In contrast, in Case 3, while the injected waterfront helps support the pressure in the production well, not a lot of water flows toward the production well, leading to a pressure drop due to reduced pressure support. The slight temperature drops of 2°C is attributed to the fact that the injected water has not yet reached production well, resulting in minimal heat exchange.

Case 4 produces similar results to Case 2, but with a lower final water production rate. This drop is due to the increased distance between the injector and production wells. In Case 4, the injected water takes longer to reach the production well because it tends to spread horizontally within the reservoir, delaying its effect on the production well's near-wellbore area.

In **Case 5**, the final water production rate is larger than in Case 3. The well spacing between the injection and production wells in Case 3 is twice as large as in Case 5. This results in the waterfront propagation in Case 5 reaching the near-wellbore area of the production wells earlier than in Case 3, leading to a higher production rate in Case 5.

The energy produced over one year of production is shown in Figure 10 for all cases. From the graph, it is evident that Case 5, with two production wells and one injection well placed 325 m apart, generates the largest energy. This is due to simultaneous production from both wells. Cases 1, and 3 show similar energy production over the year, with these two cases having both production and injection wells at the same level. Case 1, with shorter well spacing, produces more energy compared to Case 3 and 5, which have 540 m of well spacing. In contrast, Case 2 and 4, where the production and injection wells are at different levels, produce the least energy, with Case 4, having 650 m well spacing, yielding the lowest energy production. Table 3 shows the thermal energy produced and the electricity that can be produced by each case.

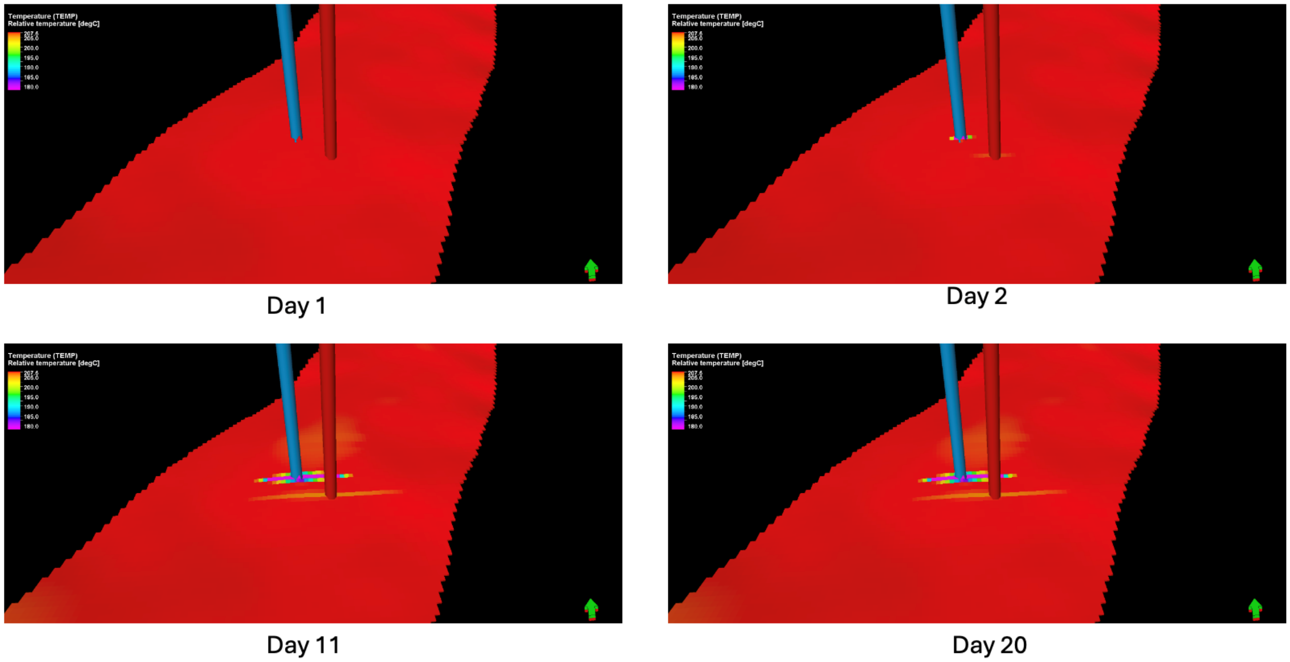

Figure 7: Temperature evolution of Case 1 during the first temperature fluctuation wave. The range of the temperature on this figure is 178 – 208 °C. The small range of temperature is to get a detailed explanation of why a small temperature drop happens on the first 11 days of production. Upper left-hand side is day 1. Upper right-hand side is the day 2. The left-hand side is day 11. Bottom right-hand side is the day 20.

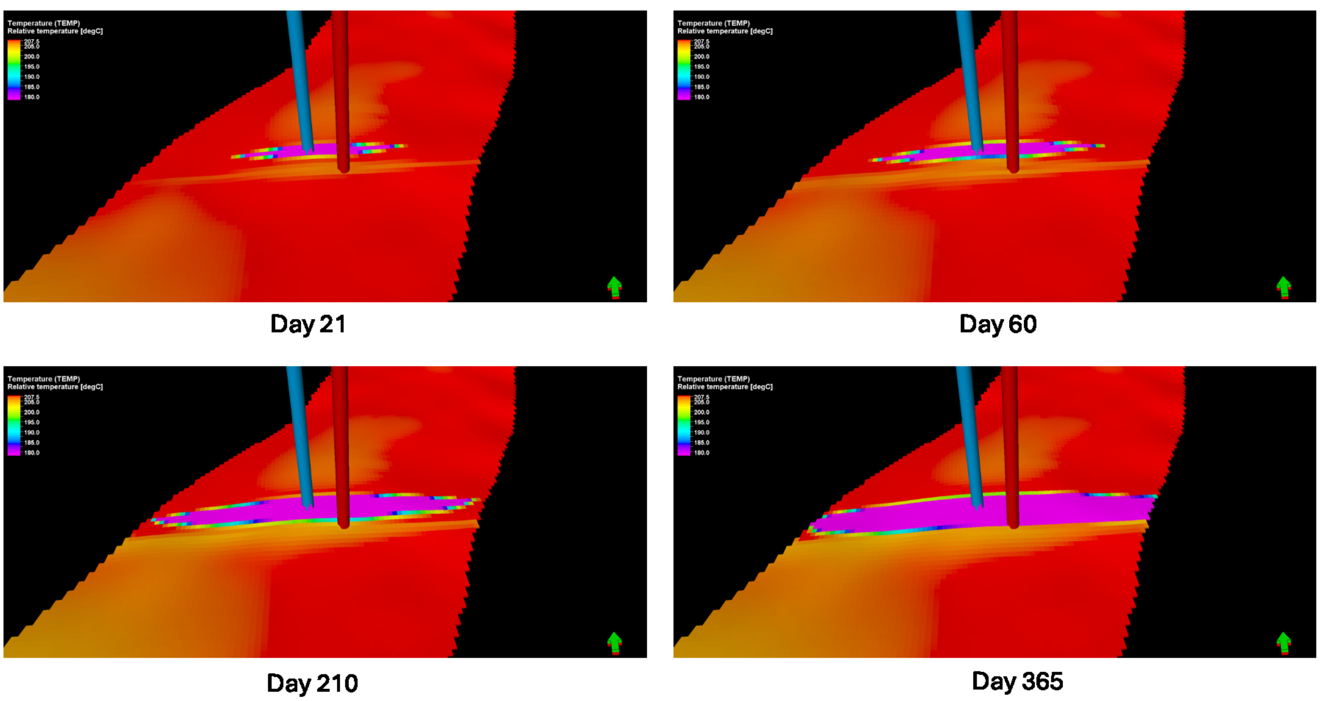

Figure 8: Temperature evolution of Case 1 during the second temperature fluctuation wave. The range of the temperature on this figure is 178 – 208 °C. From left to right to bottom day 21, day 60, day 210, and day 365.

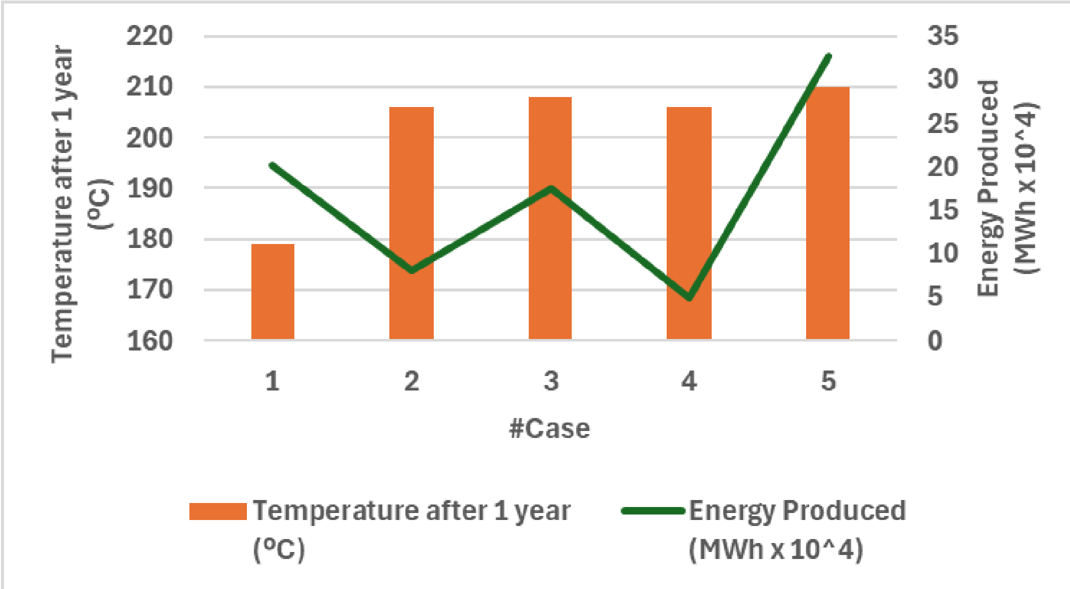

Figure 10: Temperature and cumulative energy produced for the 5 cases investigated.

Table 3: Thermal and electricity energy produced assuming a 9% conversion efficiency (based on the work of Zarrouk and Moon, 2012).

#Case	Thermal Energy Produced (MW)	Electricity Produced (MW)
1	23	2.07
2	9	0.83
3	20	1.80
4	6	0.50
5	37	3.36

6. CONCLUSION

From these results, we can conclude that the number of wells significantly impacts the energy produced. While Case 1 shows the second highest energy output, it also experiences the greatest temperature drop compared to the other cases. Over a longer production period, Case 1 is likely to produce the least energy due to the temperature decline. This warrants further investigation. Based on these findings, well perforation at different levels is not recommended for this formation.

For future research opportunities, it is recommended to explore the use of horizontal wells, consider the heterogeneity in the reservoir, and utilize actual stimulated reservoir volumes (including fractures) in the model. These modifications could reduce uncertainties in the estimated thermal performance of the basin in the RELLIS campus and provide a means to optimize geothermal energy production. Also, performing a technoeconomical analysis over longer time scales would help determine the value of additional wells (vertical or horizontal) and pumps compared to the electrical power generated.

ACKNOWLEDGMENT

The authors would like to thank Dr. Art Donovan for insights on the geology of the Brazos Basin.

REFERENCES

Bertani, R. (2016). "Geothermal Power Generation in the World 2010–2014 Update Report." *Geothermics* 60: 31-43.

Bielicki, J.M., Leveni, M., Johnson, J.X. and Ellis, B.R., 2023. The promise of coupling geologic CO2 storage with sedimentary basin geothermal power generation. *Iscience*, *26*(2).

Blackwell D, Richards M, Frone Z, Batir J, Ruzo A, Dingwall R, Williams M. Temperature-at-depth maps for the conterminous US and geothermal resource estimates. Geothermal Resources Council Transactions. 2011;35:1545-1550. Available at: https://www.osti.gov/biblio/1137036

Breede, K., Dzebisashvili, K., Liu, X. and Falcone, G., 2013. A systematic review of enhanced (or engineered) geothermal systems: past, present and future. *Geothermal Energy*, *1*, pp.1-27.

Davidoff, A.J, 1993, The Brazos Basin: Deep Basement Structure and Sediment Fill, Central East Texas, Unpublished PhD Dissertation, Texas A&M University, Department of Geology and Geophysics, 113p.

Duggal, R., Rayudu, R., Hinkley, J., Burnell, J., Wieland, C. and Keim, M., 2022. A comprehensive review of energy extraction from low-temperature geothermal resources in hydrocarbon fields. *Renewable and Sustainable Energy Reviews*, *154*, p.111865.

Elkhatat A, Al-Muhtaseb S. Climate Change and Energy Security: A Comparative Analysis of the Role of Energy Policies in Advancing Environmental Sustainability. *Energies*. 2024; 17(13):3179. https://doi.org/10.3390/en17133179

Ewing, T.E., 2001. Review of Late Jurassic depositional systems and potential hydrocarbon plays, northern Gulf of Mexico Basin.

Gallup DL. Production engineering in geothermal technology: A review. *Geothermics.* 2009;38(3):326-334. doi:10.1016/j.geothermics.2009.03.001

Gutiérrez-Negrín LCA. Evolution of worldwide geothermal power 2020–2023. *Geothermal Energy*. 2024;12:14. doi:10.1186/s40517-024-00290-w

Hook L. Geothermal energy: tapping the heat beneath our feet. *Financial Times*. Published May 3, 2021.

Hu X, Banks J, Guo Y, Liu WV. Unlocking geothermal energy by repurposing abandoned wells as enhanced geothermal systems for sustainable heat production: A numerical investigation. *J Hydrol*. 2025;651:132577. doi:10.1016/j.jhydrol.2024.132577.

Lund JW, Freeston DH, Boyd T. Geothermal Direct Use: 2010 Update. Geothermal Resources Council Transactions. 2010;34:367-372.

Lund, J. W., & Boyd, T. L. (2016). *Geothermal direct utilization: 2015 worldwide review*. Geothermics, 60, 59-64. https://doi.org/10.1016/j.geothermics.2015.11.003

National Renewable Energy Laboratory (NREL): Diversification and Energy Security. *NREL Report No. 74617*. https://www.nrel.gov/docs/fy20osti/74617.pdf

Norden, B., 2011. Geothermal energy utilization in low-enthalpy sedimentary environments.

Our World in Data. UN Population 2024 Revision. https://ourworldindata.org/un-population-2024-revision. Published 2024. Accessed January 20, 2025.

Pandey, S.N., Vishal, V. and Chaudhuri, A., 2018. Geothermal reservoir modeling in a coupled thermo-hydro-mechanical-chemical approach: a review. *Earth-Science Reviews*, *185*, pp.1157-1169.

Santos, L., Taleghani, A.D. and Elsworth, D., 2022. Repurposing abandoned wells for geothermal energy: Current status and future prospects. *Renewable Energy*, *194*, pp.1288-1302.

Sanyal, S.K., and Butler, S.J. (2006)**.** "Geothermal Power Generation." In *Geothermal Energy: Renewable Energy and the Environment* (eds. L. Dickson and M. Fanelli).

Sekar, L.K. and Okoroafor, E.R., 2024, June. Maximizing Geothermal Energy Recovery from Enhanced Geothermal Systems Through Huff-And-Puff: A Comprehensive Simulation Study. In *ARMA US Rock Mechanics/Geomechanics Symposium* (p. D022S021R001). ARMA.

Sun, W., Zhang, W., Zhao, Z. *et al.* Qualitative assessment of optimizing the well spacings based on the economic analysis. *Geotherm Energy* 12, 16 (2024). https://doi.org/10.1186/s40517-024-00295-5

Sutra, E., Spada, M. and Burgherr, P., 2017. Chemicals usage in stimulation processes for shale gas and deep geothermal systems: a comprehensive review and comparison. *Renewable and Sustainable Energy Reviews*, *77*, pp.1-11.

Tester JW, Anderson BJ, Batchelor AS, et al. *The Future of Geothermal Energy: Impact of Enhanced Geothermal Systems (EGS) on the United States in the 21st Century*. Massachusetts Institute of Technology; 2006.

Umar, Muhammad, et al. "Geothermal energy and carbon emissions nexus in leading geothermal-consuming nations: Evidence from nonparametric analysis." *Energy & Environment* 35.5 (2024): 2726-2752.

U.S. Department of Energy (DOE): Enhanced Geothermal Systems. *Office of Energy Efficiency and Renewable Energy*, https://www.energy.gov/eere/geothermal/enhanced-geothermal-systems

US Geological Survey. Assessment of high-temperature geothermal resources in hydrothermal convection systems in the United States. In: Proceedings of the 19th Intersociety Energy Conversion Engineering Conference: Advanced Energy Systems - Their Role in Our Future. LaGrange Park, IL, USA: ANS; 1984:1295-1299.

Vargas, C.A., Caracciolo, L. & Ball, P.J. Geothermal energy as a means to decarbonize the energy mix of megacities. *Commun Earth Environ* **3**, 66 (2022). https://doi.org/10.1038/s43247-022-00386-w

Weijermars, R., Burnett, D., Claridge, D., Noynaert, S., Pate, M., Westphal, D., Yu, W., & Zuo, L. (2018). Redeveloping depleted hydrocarbon wells in an enhanced geothermal system (EGS) for a university campus: Progress report of a real-asset-based feasibility study. Energy Strategy Reviews.

Wu, Yu, and Pan Li. "The potential of coupled carbon storage and geothermal extraction in a CO2-enhanced geothermal system: a review." Geothermal Energy 8.1 (2020): 19.

Zhang, S., Jiang, Z., Zhang, S., Zhang, Q. and Feng, G., 2021. Well placement optimization for large-scale geothermal energy exploitation considering nature hydro-thermal processes in the Gonghe Basin, China. *Journal of Cleaner Production*, *317*, p.128391.